

# SELECTION OF ELECTROWEAK PHYSICS HIGHLIGHTS FROM CMS: MEASUREMENTS OF TRIPLE AND QUARTIC GAUGE COUPLINGS\*

MICHAŁ SZLEPER

on behalf of the CMS Collaboration

National Center for Nuclear Research  
Pasteura 7, 02-093 Warszawa, Poland

*Received 11 March 2024, accepted 29 May 2024,  
published online 5 August 2024*

Run 2 of the LHC has produced a lot of physics results from the electroweak sector of the Standard Model. We briefly overview CMS results that relate to measurements of triple and quartic gauge couplings: diboson, vector-boson fusion, vector-boson scattering, and triboson production. We present the most recent results and activities in the field and discuss the prospects for Run 3 and beyond.

DOI:10.5506/APhysPolBSupp.17.5-A16

## 1. Introduction

The electroweak gauge sector of the Standard Model (SM) consists of two massive vector bosons,  $W$  and  $Z$ , and one massless vector boson, the photon ( $\gamma$ ); interactions between them are governed by two triple gauge couplings,  $WWZ$  and  $WW\gamma$ , and four quartic gauge couplings,  $WWWW$ ,  $WWZZ$ ,  $WWZ\gamma$ , and  $WW\gamma\gamma$ . The values of these couplings are completely determined by theory. Any deviation from the Standard Model values will result in divergences in some physical processes, which, in turn, will require new particles to regularize the high-energy behavior of the relevant amplitudes and restore unitarity in the theory. The search for anomalous couplings is equivalent to the search for new particles.

At the LHC, triple gauge couplings can be studied via the processes of diboson production and single-boson production in vector-boson fusion (VBF) mode. Quartic gauge couplings can be studied via vector-boson scattering (VBS) and triboson production.

---

\* Presented at the 30<sup>th</sup> Cracow Epiphany Conference on *Precision Physics at High Energy Colliders*, Cracow, Poland, 8–12 January, 2024.

Measurements of gauge couplings are carried out within the framework of the Standard Model Effective Field Theory (SMEFT), where non-SM interactions between known SM particles are included via additional operators of energy dimension higher than 4. Anomalous contributions to triple gauge couplings (aTGCs) are described via three CP-conserving dimension-6 operators with effective coupling constants (Wilson coefficients)  $c_{WWW}$ ,  $c_W$ , and  $c_B$  [1]. Anomalous contributions to quartic gauge couplings (aQGCs) are sought via 18 independent dimension-8 operators, with coefficients  $f_{S0}$ – $f_{S2}$ ,  $f_{M0}$ – $f_{M5}$ ,  $f_{M7}$ ,  $f_{T0}$ – $f_{T2}$ , and  $f_{T5}$ – $f_{T9}$  [2]. Higher dimension operators are suppressed by appropriate powers of  $\Lambda$ , the energy scale at which new physics explicitly shows up. This parameter sets the upper limit of the validity of the SMEFT expansion. The cross section of a process in the SMEFT formalism can be written as a coherent sum of the purely SM cross section, a  $\Lambda^{d-4}$ -suppressed SM-SMEFT interference term (where  $d$  is the dimensionality of the operator in question) and a  $\Lambda^{2(d-4)}$ -suppressed SMEFT quadratic term. One generally expects interference terms to dominate over quadratic terms.

The CMS detector is described in detail in Ref. [3].

## 2. Overview of CMS Run 2 results

### 2.1. Diboson production

The following inclusive diboson production processes were studied in Run 2:  $WW$  [4],  $WZ$  [5],  $W\gamma$  [7],  $ZZ$  [6], all the above with purely leptonic  $W$  and  $Z$  decay modes, and  $WV$ , where  $V = W, Z$ , in semileptonic decay modes [8]. All the respective cross sections were measured and compared to SM predictions calculated to NNLO or NLO accuracy in QCD. A summary of CMS results is shown in Fig. 1. Search for aTGCs is done by measuring the distributions of the dilepton mass  $m_{ll}$  for  $WW$  and the reconstructed diboson mass  $m_{VV}$  for the other processes. Processes  $WW$ ,  $WZ$ , and  $W\gamma$  are complementary in their sensitivities to aTGCs since  $WW$  probes both the  $WWZ$  and  $WW\gamma$  vertices, while  $WZ$  probes only  $WWZ$  and  $W\gamma$  probes only  $WW\gamma$ . The semileptonic  $WV$  process is by construction a combination of  $WW$  and  $WZ$ , and despite being more challenging than the purely leptonic decay modes due to hadronic background and poorer resolution, it provides fully competitive sensitivities to aTGCs. In addition, the  $ZZ$  process probes anomalous vertices  $ZZZZ$  and  $ZZ\gamma$ . Results expressed in terms of parameters  $f_4^Z$ ,  $f_4^\gamma$ ,  $f_5^Z$ , and  $f_5^\gamma$  [9] are consistent with zero within less than 0.001 (95% C.L. limit).

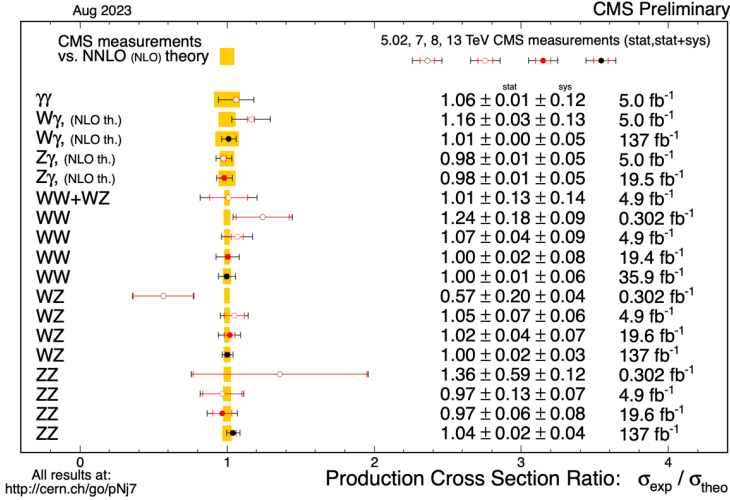


Fig. 1. Summary of CMS diboson cross sections normalized to SM predictions.

Typically, aTGC predictions are obtained by setting the cutoff parameter  $\Lambda$  to infinity (no cutoff) and by considering both SM-SMEFT interference and SMEFT quadratic terms in the calculations. Additional studies were done for the  $WZ$  process [5] to check the validity of both approaches. Limits on  $c_{WWW}$ ,  $c_W$ , and  $c_B$  were calculated as a function of the  $\Lambda$  cutoff, with  $\Lambda$  ranging from 200 GeV up to 3 TeV. Between 3 TeV and 1 TeV, limits were shown to typically loosen by a factor of  $\sim 2$ –3. Alternative aTGC limits calculated using only the interference terms revealed good sensitivity to the interference for  $c_W$  and moderate for  $c_B$ . Limits on  $c_{WWW}$  were shown to be driven almost entirely by the quadratic term. Limits were placed on individual Wilson coefficients by setting the remaining coefficients to zero, as well as allowing pairs of coefficients to vary at the same time. Studies showed little correlation between the different operators.

The interference issue has been revisited in a more recent analysis of inclusive  $W\gamma$  production [10]. By looking at the distribution of the azimuthal angle  $\phi$  of the positive helicity lepton (positive charged lepton or antineutrino) in the  $W\gamma$  center-of-mass frame, following the suggestion of theoretical work [11], sensitivity to the interference term was shown to increase by an order of magnitude for  $c_{WWW}$ . While the quadratic term still plays an important role, it is possible to obtain reasonably stringent limits on  $c_{WWW}$  from the interference term alone.

A summary of CMS aTGCs searches, including Run 1 and Run 2 data, is shown in Fig. 2. Overall, good agreement with the SM is found.

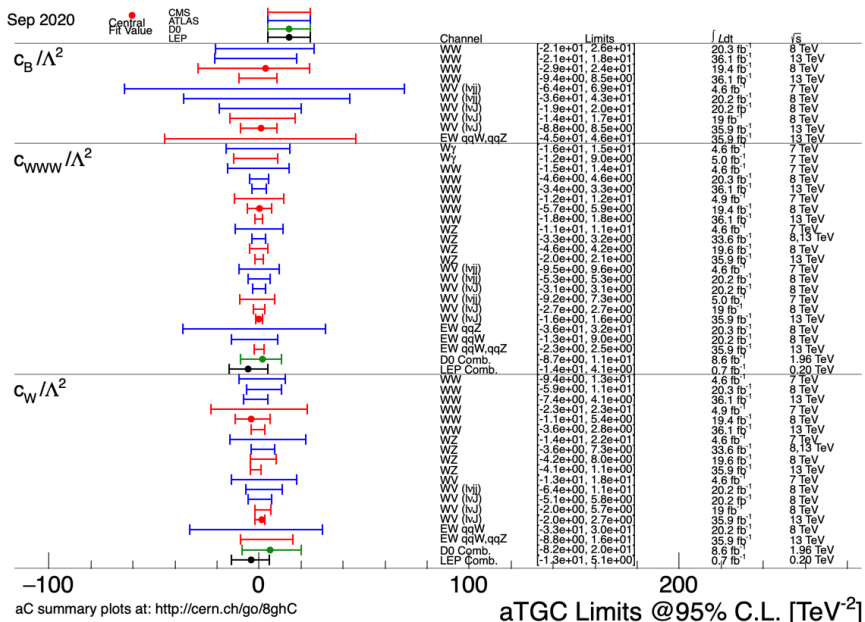


Fig. 2. Summary of CMS 95% C.L. limits on dimension-6 SMEFT parameters  $c_B$ ,  $c_{WWW}$ , and  $c_W$ .

## 2.2. Single-boson production in VBF mode

The smoking gun signature of VBF is two highly energetic “tagging” jets, with a large separation in pseudorapidity  $\Delta\eta_{jj}$  and high dijet mass  $m_{jj}$ . Processes  $W + 2$  jets [12] and  $Z + 2$  jets [13] provide additional tests of the SM and constraints on aTGCs. The former probes both  $WWZ$  and  $WW\gamma$ , the latter probes only the  $WWZ$  vertex. Anomalous contributions are searched for by measuring the distributions of transverse momenta of the lepton coming from  $W$  decay,  $p_T^l$ , and of the  $Z$  boson,  $p_T^Z$ , respectively. Results, included in Figs. 2 and 3, are consistent with the Standard Model predictions and obtained 95% C.L. limits on aTGCs are competitive with those from diboson for  $c_{WWW}$  and somewhat less stringent for  $c_W$  and  $c_B$ .

## 2.3. Vector-boson scattering

The VBS signal is formally defined as electroweak-diboson production with at least two additional “tagging” jets, with a large  $\Delta\eta_{jj}$  and a high  $m_{jj}$ , suggestive of a hard boson–boson interaction. These processes provide the best probe of quartic gauge couplings. Table 1 shows the SM and non-SM couplings probed by each VBS process.

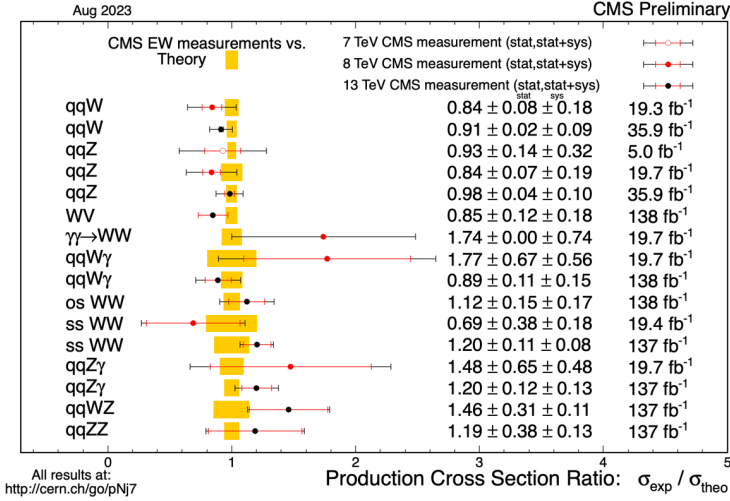


Fig. 3. Summary of CMS VBF and VBS cross sections normalized to the SM predictions.

Table 1. VBS processes sorted by final state and the quartic couplings they probe.

VBS process	SM couplings	Non-SM couplings
Same-sign $WW$	$WWWW$	—
Opposite-sign $WW$	$WWWW, WWZZ, WW\gamma\gamma, WWZ\gamma$	—
$WZ$	$WWZZ, WWZ\gamma$	—
$ZZ$	$WWZZ$	$ZZZZ, ZZZ\gamma, ZZ\gamma\gamma$
$W\gamma$	$WW\gamma\gamma, WWZ\gamma$	—
$Z\gamma$	$WWZ\gamma$	$ZZZ\gamma, ZZ\gamma\gamma, Z\gamma\gamma\gamma$
$\gamma\gamma$	$WW\gamma\gamma$	$ZZ\gamma\gamma, Z\gamma\gamma\gamma, \gamma\gamma\gamma\gamma$

The following VBS processes have been studied in CMS: the same-sign  $WW$  [14],  $WZ$  [15],  $ZZ$  [16],  $W\gamma$  [17],  $Z\gamma$  [18], all with leptonic  $W$  and  $Z$  decays, and the semileptonic  $VV$  [19] which includes the same-sign  $WW$ , the opposite-sign  $WW$ ,  $WZ$ , and  $ZZ$  (for the final cross-section measurement only  $WW$  and  $WZ$  were used). VBS signal has been observed with a significance of more than 5 standard deviations (s.d.) for the same-sign  $WW$ ,  $WZ$ ,  $Z\gamma$ , and most recently  $W\gamma$ . A 4 s.d. evidence was obtained for  $ZZ$  and 4.4 s.d. for  $VV$ . Measured cross sections, including those from Run 1, are summarized in Fig. 3. Agreement with the SM is good.

Searches for aQGCs were performed based on the measured distributions of the reconstructed total diboson mass  $m_{VV}$  or of the transverse mass  $m_{\text{T}}^{VV}$  (for  $WW$  and optionally  $WZ$ ). Upper limits were placed on Wilson coefficients of dimension-8 operators:  $f_{S0}$ ,  $f_{S1}$ ,  $f_{T0-fT2}$ ,  $f_{M0}$ ,  $f_{M1}$ ,  $f_{M7}$  from the same-sign  $WW$ ,  $WZ$  and  $VV$ ,  $f_{T0-fT2}$ ,  $f_{T8}$ ,  $f_{T9}$  from  $ZZ$ ,  $f_{M0-fM5}$ ,  $f_{M7}$ ,  $f_{T0-fT2}$ ,  $f_{T5-fT7}$  from  $W\gamma$ , and  $f_{M0-fM5}$ ,  $f_{M7}$ ,  $f_{T0-fT2}$ ,  $f_{T5-fT9}$  from  $Z\gamma$ . Therefore, all the relevant dimension-8 operators have been experimentally constrained (including  $f_{S2}$  which in the same-sign  $WW$  has the same effect as  $f_{S0}$ ). Measurements coming from different processes are complementary. The most stringent limits on  $f_{S0}$ ,  $f_{S1}$ ,  $f_{T0-fT2}$ ,  $f_{M0}$ ,  $f_{M1}$ , and  $f_{M7}$  come from  $VV$  followed by the same-sign  $WW$ ,  $f_{M2-fM5}$  and  $f_{T5-fT7}$  are best constrained by  $W\gamma$ , while  $f_{T8}$  and  $f_{T9}$  require study of  $ZZ$  and  $Z\gamma$ .

As it was for aTGCs, the baseline procedure in aQGC searches assumed an infinite value of the cutoff parameter  $\Lambda$ . An additional study was done for the same-sign  $WW$ ,  $WZ$ , and their combination. Here, the ‘‘partial clipping’’ technique was applied: generated distributions of the diboson mass in the aQGC scenarios were clipped at the energy corresponding to the lowest unitarity limit which is relevant to the studied process, only SM contributions were allowed above this value; aQGC predictions were recalculated accordingly. Limits on dimension-8 operators obtained using this technique were typically weaker by a factor 4–5 than those calculated without clipping. All aQGC predictions were calculated using both interference terms as well as quadratic terms. Finally, limits were calculated for individual Wilson coefficients, setting all the remaining coefficients to zero, including those of dimension-6 operators.

Final-state polarizations were also studied in the same-sign  $WW$  process [20]. The analysis involved exploiting tiny differences in the final-state kinematics between longitudinal and transverse  $W$ -boson polarizations, including such variables as the azimuthal separation of the two jets  $\Delta\phi_{jj}$  and of the two leptons  $\Delta\phi_{ll}$ , as well as  $m_{ll}$ . First hints of the existence of longitudinal polarizations were observed with a significance of 2.3 s.d., consistent with SM expectations.

#### 2.4. Recent VBS and aQGC related activities

In a recent analysis, the first observation of VBS signal in the opposite-sign  $WW$  process was reported [21]. Advanced deep neural network techniques were applied, with kinematic inputs from  $m_{jj}$ ,  $\Delta\eta_{jj}$ ,  $\Delta\phi_{ll}$ , transverse momenta of the tagging jets  $p_{\text{T}}^j$  and of the dilepton system  $p_{\text{T}}^{ll}$ , the Zeppenfeld variable  $z_l$  for both leptons and the transverse mass of the leading lepton  $m_{\text{T}}^{l1}$ . This together with data-driven background normalization techniques and background control regions, allowed for the extraction of a VBS signal

with a significance of 5.6 s.d. (5.2 expected). Measured cross sections are consistent with the SM predictions (and included in Fig. 3). The opposite-sign  $WW$  process has more sensitivity to Higgs and triple gauge couplings than its same-sign counterpart, via additional diagrams in the  $s$ -channel. It can be used in a future combination of channels to improve limits on dimension-6 operators.

Another recent development in CMS and a possible path for further improvements is the inclusion of  $\tau$  decay channels. A recent analysis of the same-sign  $WW$  process [22] considered final leptonic states consisting of one light lepton (electron or muon) and one tau lepton decaying into hadrons. To identify hadronic taus, a deep neural network was used with inputs from  $m_{jj}$ ,  $m_{\tau}^l$ , transverse momenta  $p_{\text{T}}^j$ ,  $p_{\text{T}}^{\tau}$ ,  $p_{\text{T}}^l$ , and two mass-like variables defined as

$$M_{\text{IT}}^2 = \left( \sqrt{m_{\tau l}^2 + p_{\text{T}}^{\tau l^2} + p_{\text{T}}^{\text{miss}} \right)^2 - \left| \vec{p}_{\text{T}}^{\tau l} + \vec{p}_{\text{T}}^{\text{miss}} \right|^2, \quad (1)$$

and

$$M_{\text{ol}}^2 = \left( p_{\text{T}}^{\tau} + p_{\text{T}}^l + p_{\text{T}}^{\text{miss}} \right)^2 - \left| \vec{p}_{\text{T}}^{\tau} + \vec{p}_{\text{T}}^l + \vec{p}_{\text{T}}^{\text{miss}} \right|^2 \quad (2)$$

useful to signal a VBS interaction. The observed signal significance was 2.7 s.d.

Quartic vertices with two photons, like  $WW\gamma\gamma$  or the anomalous  $ZZ\gamma\gamma$ , can be also probed using a different technique. Instead of requiring two tagging jets, we can require two intact scattered protons. These can be detected using the Precision Proton Spectrometer (PPS), a system of tracking devices very close to the beamline, located some 200 meters away from the main CMS detector. In the central detector, we look for two highly energetic acoplanar fat jets with large 2-subjettiness, suggestive of a pair of hadronically decayed  $W$  or  $Z$  bosons. The presence of scattered protons in the PPS suggests interaction via photon radiations. Protons in the PPS are matched with jets in the central detector via their respective invariant masses and rapidities. Using this technique, upper limits have been placed on the respective cross sections  $\sigma(pp \rightarrow pWWp)$  and  $\sigma(pp \rightarrow pZZp)$  [23]. These measurements translate into limits on dimension-8 operators  $f_{M0}$ – $f_{M7}$ . The obtained precision on  $f_{M2}$  is comparable with that obtained from other processes, in particular,  $Z\gamma$ ; for other Wilson coefficients, it is significantly weaker. However, such measurements can provide valuable cross checks of consistency.

### 2.5. Triboson production

Triboson production processes offer an independent way to study quartic gauge couplings. They are, however, even more challenging due to very low

cross sections, low leptonic branching fractions, and complicated combinatorics. The following triboson production processes have been studied in CMS:  $WWW$ ,  $WWZ$ ,  $WZZ$ ,  $ZZZ$  [24],  $W\gamma\gamma$ ,  $Z\gamma\gamma$  [25], and most recently  $WW\gamma$  [26].

A 5 s.d. observation was reported for the total  $VVV$  production, where  $V = W, Z$ , but only  $WWW$  exceeds 3 s.d. significance on its own. An upper limit was placed on  $ZZZ$  production based on a null observation in consistency with SM expectations. Reported signal significances for  $W\gamma\gamma$ ,  $Z\gamma\gamma$ , and  $WW\gamma$  are 3.1, 4.8, and 5.6 s.d., respectively. A summary of the measured cross sections is presented in Fig. 4.

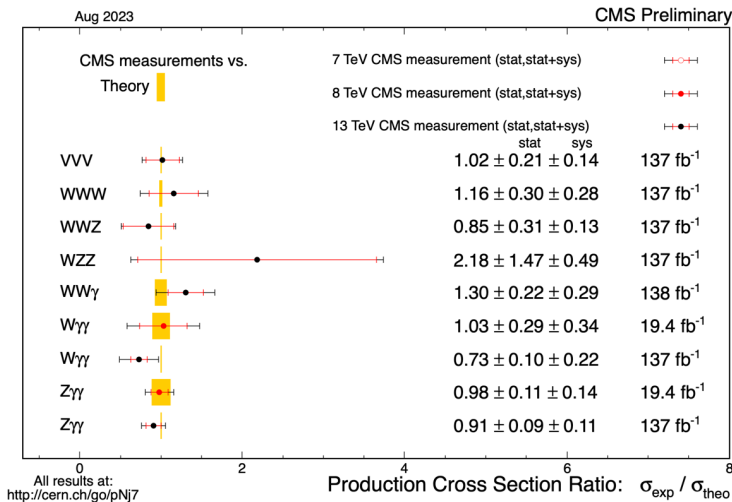


Fig. 4. Summary of CMS triboson cross sections normalized to the SM predictions.

Searches for aQGCs were conducted in  $WWW$ ,  $W\gamma\gamma$ , and  $Z\gamma\gamma$  processes. Obtained limits are usually less stringent than those from VBS, although limits on  $f_{T5}$ – $f_{T7}$  obtained from  $W\gamma\gamma$  and on  $f_{T8}$  and  $f_{T9}$  from  $Z\gamma\gamma$  are significant.

### 3. Summary and prospects for Run 3 and beyond

Run 2 has produced a lot of results from the electroweak gauge sector. This includes: diboson production cross sections for  $WW$ ,  $WZ$ ,  $ZZ$ ,  $W\gamma$ ,  $WV$  (semileptonic), single-boson production with 2 jets (VBF) for both  $W$  and  $Z$ , electroweak diboson with 2 jets (VBS) cross sections for the same-sign  $WW$ ,  $WZ$ ,  $ZZ$ ,  $W\gamma$ ,  $Z\gamma$ , semileptonic  $VV$  and the opposite-sign  $WW$ , triboson production cross sections for  $VVV$ ,  $W\gamma\gamma$ ,  $Z\gamma\gamma$ , and  $WW\gamma$ . Multiple constraints have been placed on aTGCs as well as aQGCs — upper limits



have been placed on  $c_{WWW}$ ,  $c_W$ ,  $c_B$ , and on all the relevant 18 dimension-8 operators. It is clear that measurements of triple and quartic gauge couplings will benefit from increased statistics from Run 3, and in the longer term, from the HL-LHC phase. For many of the abovementioned analyses, in particular the same-sign  $WW$ ,  $WZ$  and massive triboson production, sheer statistics is still the main limiting factor. Improving precision will be more challenging for processes with a high QCD-induced background. Extraction of the pure electroweak cross section relies largely on calculations. Input will be needed also from the theory side.

Many improvements can be expected in the interpretation of results in the SMEFT language. It has been shown that observing the SMEFT validity region defined by parameter  $\Lambda$  is imperative for dimension-8 operators, especially for processes involving massive vector bosons. The most complete and correct way of placing limits on SMEFT coefficients is as a function of  $\Lambda$ , with  $\Lambda$  varying between an arbitrary low value (of course, if new physics was present at a very low scale, we would have already seen it!) and the relevant unitarity limit. The unitarity condition defines the maximum value of any Wilson coefficient that is physically allowed for a given value of  $\Lambda$ . We can place physically meaningful limits only as long as they are stricter than limits dictated solely by the unitarity condition. The same considerations apply also to aTGCs and dimension-6 operators, although due to a milder energy dependence, these issues are here less crucial.

Relative contributions from interference and quadratic terms have never been studied in CMS for dimension-8 operators. To facilitate physics interpretation, calculation of limits with and without quadratic terms is strongly encouraged. Novel ways to improve sensitivity to the interference may be required, *e.g.*, by looking at angular correlations between physics objects in addition to mass-related variables. Applying Machine Learning techniques to use many kinematic inputs simultaneously can be very beneficial both for dimension-6 and dimension-8 operators.

Finally, an important long-term milestone will be to move beyond the one-operator-at-a-time scheme. For aTGCs, correlated 2-dimensional limits have already been set, the number of independent parameters is small and correlations are moderate. This represents a much bigger issue for aQGCs, where the number of parameters is large and many of them are known to be highly correlated (*e.g.*,  $f_{S0}$  and  $f_{S1}$ ). As already hinted by the semileptonic analyses, a combination of processes may be an effective way to increase precision and decorrelate different parameters. Moreover, VBS data, *e.g.*, the opposite-sign  $WW$ , can be used in combination with non-VBS processes to improve constraints on dimension-6 operators.

Clearly, there is a long road ahead of us. The most interesting results are yet to come.

This research was partially funded by a grant from the National Science Center (NCN), Poland, contract No. 2021/41/B/ST2/01369.

## REFERENCES

- [1] C. Degrande *et al.*, *Ann. Phys.* **335**, 21 (2013), [arXiv:1205.4231 \[hep-ph\]](#); B. Grzadkowski, M. Iskrzyński, M. Misiak, J. Rosiek, *J. High Energy Phys.* **2010**, 085 (2010), [arXiv:1008.4884 \[hep-ph\]](#).
- [2] O.J.P. Éboli, M.C. Gonzalez-Garcia, J.K. Mizukoshi, *Phys. Rev. D* **74**, 073005 (2006), [arXiv:hep-ph/0606118](#); O.J.P. Éboli, M.C. Gonzalez-Garcia, *ibid.* **93**, 093013 (2016), [arXiv:1604.03555 \[hep-ph\]](#).
- [3] CMS Collaboration, *J. Instrum.* **3**, S08004 (2008).
- [4] CMS Collaboration, *Phys. Rev. D* **102**, 092001 (2020), [arXiv:2009.00119 \[hep-ex\]](#).
- [5] CMS Collaboration, *J. High Energy Phys.* **2019**, 122 (2019), [arXiv:1901.03428 \[hep-ex\]](#); *ibid.* **2022**, 031 (2022), [arXiv:2110.11231 \[hep-ex\]](#).
- [6] CMS Collaboration, *Eur. Phys. J. C* **78**, 165 (2018), [arXiv:1709.08601 \[hep-ex\]](#); *ibid.* **81**, 200 (2021), [arXiv:2009.01186 \[hep-ex\]](#).
- [7] CMS Collaboration, *Phys. Rev. Lett.* **126**, 252002 (2021), [arXiv:2102.02283 \[hep-ex\]](#).
- [8] CMS Collaboration, *J. High Energy Phys.* **2019**, 062 (2019), [arXiv:1907.08354 \[hep-ex\]](#).
- [9] K. Hagiwara, R.D. Peccei, D. Zeppenfeld, *Nucl. Phys. B* **282**, 253 (1987).
- [10] CMS Collaboration, *Phys. Rev. D* **105**, 052003 (2022), [arXiv:2111.13948 \[hep-ex\]](#).
- [11] G. Panico, F. Riva, A. Wulzer, *Phys. Lett. B* **776**, 473 (2018), [arXiv:1708.07823 \[hep-ph\]](#); A. Azatov, D. Barducci, E. Venturini, *J. High Energy Phys.* **2019**, 075 (2019), [arXiv:1901.04821 \[hep-ph\]](#).
- [12] CMS Collaboration, *Eur. Phys. J. C* **80**, 43 (2020), [arXiv:1903.04040 \[hep-ex\]](#).
- [13] CMS Collaboration, *Eur. Phys. J. C* **78**, 589 (2018), [arXiv:1804.05252 \[hep-ex\]](#).
- [14] CMS Collaboration, *Phys. Rev. Lett.* **120**, 081801 (2018), [arXiv:1709.05822 \[hep-ph\]](#); *Phys. Lett. B* **809**, 135710 (2020), [arXiv:2005.01173 \[hep-ph\]](#).
- [15] CMS Collaboration, *Phys. Lett. B* **795**, 281 (2019), [arXiv:1901.04060 \[hep-ph\]](#), see also Ref. [14] above.
- [16] CMS Collaboration, *Phys. Lett. B* **774**, 682 (2017), [arXiv:1708.02812 \[hep-ph\]](#), *ibid.* **812**, 135992 (2020), [arXiv:2008.07013 \[hep-ex\]](#).

- [17] CMS Collaboration, *Phys. Lett. B* **811**, 135988 (2020),  
[arXiv:2008.10521 \[hep-ex\]](#); *Phys. Rev. D* **108**, 032017 (2023),  
[arXiv:2212.12592 \[hep-ex\]](#).
- [18] CMS Collaboration, *J. High Energy Phys.* **2020**, 076 (2020),  
[arXiv:2002.09902 \[hep-ex\]](#); *Phys. Rev. D* **104**, 072001 (2021),  
[arXiv:2106.11082 \[hep-ex\]](#).
- [19] CMS Collaboration, *Phys. Lett. B* **798**, 134985 (2019),  
[arXiv:1905.07445 \[hep-ex\]](#); *ibid.* **834**, 137438 (2022),  
[arXiv:2112.05259 \[hep-ex\]](#).
- [20] CMS Collaboration, *Phys. Lett. B* **812**, 136018 (2021),  
[arXiv:2009.09429 \[hep-ex\]](#).
- [21] CMS Collaboration, *Phys. Lett. B* **841**, 137495 (2023),  
[arXiv:2205.05711 \[hep-ex\]](#).
- [22] CMS Collaboration, CMS-PAS-SMP-22-008 (Public Analysis Summary).
- [23] CMS Collaboration, *J. High Energy Phys.* **2023**, 229 (2023),  
[arXiv:2211.16320 \[hep-ex\]](#).
- [24] CMS Collaboration, *Phys. Rev. D* **100**, 012004 (2019),  
[arXiv:1905.04246 \[hep-ex\]](#); *Phys. Rev. Lett.* **125**, 151802 (2020),  
[arXiv:2006.11191 \[hep-ex\]](#).
- [25] CMS Collaboration, *J. High Energy Phys.* **2021**, 174 (2021),  
[arXiv:2105.12780 \[hep-ex\]](#).
- [26] CMS Collaboration, *Phys. Rev. Lett.* **132**, 121901 (2024),  
[arXiv:2310.05164 \[hep-ex\]](#).